Quantitative Analysis of Monovalent Counterion Binding to Random-Sequence, Double-Stranded DNA Using the Replacement Ion Method†

Earle Stellwagen, Qian Dong,‡ and Nancy C. Stellwagen*

Department of Biochemistry, University of Iowa, Iowa City, Iowa 52242

Received October 12, 2006; Revised Manuscript Received December 1, 2006

ABSTRACT: A variation of affinity capillary electrophoresis, called the replacement ion (RI) method, has been developed to measure the binding of monovalent cations to random sequence, double-stranded (ds) DNA. In this method, the ionic strength is kept constant by gradually replacing a non-binding ion in the solution with a binding ion and measuring the mobility of binding and non-binding analytes as a function of binding ion concentration. The method was validated by measuring the binding of Li^+ ions to adenosine nucleotides; the apparent dissociation constants obtained by the RI method are comparable to literature values obtained by other methods. The binding of $Tris^+$, NH_4^+, Li^+, Na^+, and K^+ to dsDNA was then investigated. The apparent dissociation constants observed for counterion binding to a random-sequence 26-base pair (bp) oligomer ranged from 71 mM for $Tris^+$ to 173 mM for Na^+ and K^+. Hence, positively charged Tris buffer ions will compete with other monovalent cations in Tris-buffered solutions. The bound cations identified in this study may correspond to the strongly correlated, tightly bound ions recently postulated to exist as a class of ions near the surface of dsDNA (Tan, Z.-J., and Chen, S.-J. (2006) *Biophys. J. 91,* 518−536). Monovalent cation binding to random-sequence dsDNA would be expected to occur in addition to any site-specific binding of cations to A-tracts or other DNA sequence motifs. Single-stranded DNA oligomers do not bind the five tested cations under the conditions investigated here.

The binding of monovalent cations to DNA and other polynucleotides has been studied for many years. Early free boundary electrophoresis and conductivity studies (*1*−*3*) showed that the affinity of cations for calf thymus DNA decreases in the order $Li^+ > Na^+ > K^+ \gg$ tetramethylammonium (TMA^{+1}). Competitive dialysis measurements (*4*) showed that Li^+, Na^+, K^+, Cs^+, and tetrabutylammonium (TBA^+) ions bind to double-stranded (ds) DNA in a sequence-independent manner, whereas TMA^+ and tetraethylammonium (TEA^+) ions are preferentially bound by AT-rich DNAs. ^{23}Na NMR measurements (*5*) showed that Na^+, TEA^+, and TBA^+ bind to DNA with relative affinities of 20:5:1, respectively. Tris(hydroxymethyl)aminomethane ($Tris^+$) ions also bind to DNA, with an affinity similar to that observed for Na^+ (*5*).

More recently, Korolev et al. (*6*), studying the X-ray diffraction of oriented B-DNA fibers, found that the binding affinity decreases as Na^+, $K^+ > Li^+$, opposite to the order observed in aqueous solution. Tikhomirova and Chalikian (*7*), using ultrasonic velocimetry, found that Li^+, Na^+, K^+, Rb^+, Cs^+, NH_4^+, and TMA^+ ions retain their full hydration shells when bound to polydG·polydC and polydI·polydC, but are dehydrated when bound to polydA·polydT, suggesting site-specific binding in the latter case. Gearheart et al. (*8*), using ultrafast time-resolved Stokes-shift spectroscopy, found that Na^+ interacts specifically with a random-sequence DNA oligomer, whereas TBA^+ does not. Finally, Ouameur et al. (*9*), using FTIR and UV spectroscopy, found that thallium binds to calf thymus DNA with an apparent dissociation constant of 71 μM. They also found that cation binding increases with increasing cation concentration.

The site-specific binding of monovalent cations to DNA A-tracts, runs of 5−6 contiguous adenine residues, has also been studied. X-ray diffraction (*10*−*14*), NMR (*15*−*20*), fluorescence resonance energy transfer (*21*), and electrophoresis (*22*, *23*) measurements, along with molecular dynamics simulations (*24*−*32*), have suggested that monovalent counterions are preferentially localized in the narrow minor grooves of A-tracts, providing a rationale for the A-tract-induced curvature of the DNA helix axis (*33*−*36*). Other theoretical (*37*, *38*) and experimental (*39*−*41*) studies have also led to the conclusion that asymmetric counterion binding can induce modest but significant time-averaged effects on DNA conformation.

Monovalent cations bind to nucleotides as well as to DNA (*42*−*44*). Various studies have shown, for example, that 5′-adenosine triphosphate (ATP), 5′-adenosine diphosphate (ADP), and 5′-adenosine monophosphate (AMP) bind alkali metal ions with apparent dissociation constants ranging from 20 to 600 mM, depending on the particular cation−nucleotide

† This work was supported in part by the National Institute of General Medical Sciences (GM061009).

* Corresponding author. Tel: (319) 335-7896. Fax: (319) 335-9570. E-mail: nancy-stellwagen@uiowa.edu.

‡ Present address: Department of Internal Medicine, University of Iowa, Iowa City, IA 52242.

[1] Abbreviations: A-COOH, 5′-adenosine carboxylic acid; ADP, 5′-adenosine diphosphate; AMP, 5′-adenosine monophosphate; cAMP, 3′,5′-cyclic AMP; ATP, 5′-adenosine triphosphate; ds26, 26-base pair double-stranded DNA; CE, capillary electrophoresis; DM, diethylmalonate; PAGE, polyacrylamide gel electrophoresis; RI, replacement ion; ss5, 5-nucleotide single-stranded DNA; ss26, 26-nucleotide single-stranded DNA; TMA, tetramethylammonium; TEA, tetraethylammonium; TPA, tetrapropylammonium; TBA, tetrabutylammonium.

10.1021/bi062132w CCC: $37.00
Published on Web 01/25/2007

pair (*43*, *44* and references therein). The binding affinities increase with increasing number of phosphate residues in the nucleotide and decrease with the increasing radius of the bound cation, as expected for an electrostatic interaction between an analyte and ligand (*43*, *45*). $Tris^+$ buffer ions also bind to the adenosine nucleotides, with apparent dissociation constants similar to those observed for Li^+ (*44*). Because $Tris^+$ and Li^+ differ markedly in size, the binding of $Tris^+$ probably occurs through a combination of hydrogen bonds and electrostatic interactions (*44*, *45*). 5′-Adenosine carboxylic acid (A-COOH) and 3′-5′-cyclic AMP (cAMP) do not bind monovalent cations (*44*), suggesting that two or more closely spaced oxyanions are required for monovalent cation binding to mononucleotides.

The studies described in this article were designed to determine whether monovalent cations bind in a similar manner to random-sequence DNA and, if so, to measure the binding affinities. To evaluate cation binding, we have developed a variation of affinity capillary electrophoresis (see refs 46 and 47 (*46*, *47*) for a general discussion of the technique) called the Replacement Ion (RI) method. In this method, the ionic strength of the solution is kept constant by gradually replacing a non-binding ion in the solution with a test ion; the mobility of the analyte−ligand complex is measured as a function of test ion concentration. Because the ionic strength of the solution remains constant, the continual decrease of electrophoretic mobility with increasing ionic strength (*48*−*51*) does not affect the observed mobilities. Corrections for differences in the intrinsic conductivities of the binding and non-binding ions are made by including a non-binding analyte in each solution. Apparent dissociation constants are calculated by nonlinear curve fitting of the difference mobility profiles, assuming only that the on/off binding reaction is rapid and that the analyte and its ligand-bound complex have measurably different mobilities. The RI method was validated by measuring the binding of Li^+ to ATP, ADP, and AMP; the apparent dissociation constants are comparable to other values in the literature, obtained by different methods.

The RI method was then used to measure the binding of monovalent cations to two double-stranded (ds) DNAs, linear pUC19 (2686 bp) and a random-sequence 26 bp oligomer. Single-stranded (ss) DNA oligomers containing 5 and 26 nucleotides were also characterized. The test ions were Li^+, Na^+, K^+, NH_4^+, and $Tris^+$; several different quaternary ammonium ions were used as non-binding ions. Na^+ and K^+ were chosen as test ions because of their biological relevance, Li^+ and NH_4^+ were chosen because they bind to nucleotides (*42*, *43*, *45*), and $Tris^+$ was chosen because Tris buffers are frequently used to maintain neutral pH in biochemical reactions carried out *in vitro*. The results indicate that the five tested monovalent cations bind weakly to dsDNA, with apparent dissociation constants in the range of ∼100 mM. The cations do not bind significantly to ssDNA under the conditions used here.

MATERIALS AND METHODS

Samples. DNA oligomers containing 5 and 26 nucleotides (nt) were synthesized by Integrated DNA Technologies (Coralville, IA) and purified by HPLC or polyacrylamide gel electrophoresis (PAGE). The oligomers had the expected molecular weights when measured by matrix-associated laser desorption ionization time-of-flight (MALDI-TOF) mass spectrometry and migrated as single, sharp peaks during capillary electrophoresis (CE). The 5-nt oligomer, called ss5 for brevity, had the sequence ACCGT; the sequence of one of the 26-nt oligomers (called ss26) was 5′-CGCAGTG-TACGACTAGACTACAGACG. The double-stranded 26-bp oligomer (called ds26) was prepared by heating equimolar concentrations of ss26 and its complement in 10 mM Tris-Cl buffer, pH 8.0, to 94 °C for 5 min and cooling slowly to room temperature. The duplex was monodisperse when analyzed by PAGE and CE. Plasmid pUC19 (2686 bp, Invitrogen, Carlsbad, CA) was linearized by digestion with the blunt-cutting enzyme *Sma*I; the linearized plasmid was monodisperse when analyzed by PAGE. Stock solutions containing ∼30 ng/μL (∼0.05 mM bp) of each DNA in 10 mM Tris-Cl buffer were stored at −20 °C until needed. ATP, ADP, AMP, cAMP, and A-COOH were reagent grade chemicals (Sigma Chemical Co., St. Louis, MO) used without further purification. The nucleotides were dissolved in deionized water (Nanopure II, Barnstead International, Dubuque, IA) at a concentration of 0.05 μg/μL and stored at −20 °C.

Buffers. All CE experiments were carried out in solutions containing 200 mM diethylmalonic acid (DM), titrated to pH 7.3, the pK_a of the second carboxyl group, with concentrated solutions of the hydroxide or amine of the cation of interest. Because the second carboxyl group of diethylmalonate is half ionized at pH 7.3, the concentration of the cation(s) in each solution was 300 mM; the ionic strength was 400 mM. This buffer concentration was chosen as a compromise between having enough cations in the solution to measure the affinity and keeping the conductivity of the solution low enough to avoid Joule heating in the capillary. Because the anion is the buffering ion, the cation may be changed at will without altering the pH or buffering capacity of the solution.

The cations used in the conductivity experiments described below included the alkali metal ions Li^+, Na^+, K^+, and Rb^+; the partially substituted ammonium ions $MeNH_3^+$, Me_3NH^+, $EtNH_3^+$, and $Tris^+$; and the tetraalkylammonium ions Me_4N^+, Et_4N^+, Pr_4N^+, and Bu_4N^+, where Me, Et, Pr, and Bu represent the methyl, ethyl, *n*-propyl, and *n*-butyl groups, respectively. For brevity, the tetraalkylammonium ions are abbreviated TMA^+, TEA^+, TPA^+, and TBA^+, respectively, in the following text. Quantitative binding studies were carried out using Li^+, Na^+, K^+, NH_4^+, and $Tris^+$ as the test ions. Mixed cation-tetraalkylammonium solutions with the desired compositions were prepared by combining appropriate quantities of the individual stock solutions. Diethylmalonic acid, $[(CH_3CH_2)_2C(COOH)_2]$, was purchased from Sigma-Aldrich (St. Louis, MO). Other chemicals were obtained from Fisher Scientific (Fair Lawn, NJ), Research Products International (Mt. Prospect, IL), Eastman Kodak (Rochester, NY), or Fluka (Steinheim, Germany). The pH of each buffer solution was measured with a Radiometer PHM82 Standard Meter (Copenhagen).

Capillary Electrophoresis. Capillary zone electrophoresis measurements were carried out with a Beckman Coulter P/ACE MDQ Capillary Electrophoresis System (Fullerton, CA), run in the reverse polarity mode (anode on the detector side) with UV detection at 254 nm, using methods described

previously (*52*). Migration times and peak areas were analyzed using the 32 Karat software. Bio-Rad (Hercules CA) LPA capillaries, coated internally with linear polyacrylamide, were used to minimize the electroosmotic flow (EOF) of the solvent. Previous studies have shown that the capillary coating does not affect the observed mobilities (*52*). The capillaries were 40.0 cm in length (29.8 cm to the detector) and had external diameters of 375 μm and internal diameters of 75 μm. The capillary was conditioned at the beginning of each day by rinsing with running buffer for 5 min at high pressure (25 psi, 0.17 Mpa). The capillary was rinsed with deionized water at 25 psi for 5−10 min at the end of each day and stored in deionized water. The capillary cartridge was cooled with circulating liquid; the temperature of all experiments was 20.0 ± 0.1 °C. The samples were hydrodynamically injected into the capillary by applying low pressure (0.5 psi, 0.0035 MPa) for 3 s. The injection volume was 22 nL; the length of the sample plug was 0.51 cm, 1.3% of the total capillary length. The electric field strength was typically 150−200 V/cm (6−8 kV applied voltage); the current was ≤60 μA. Control experiments showed that the observed mobilities were independent of the applied electric field, the length of the sample plug, and DNA concentration.

The residual EOF of the capillary was measured frequently by the fast method of Williams and Vigh (*53*), using 40 mM acrylamide or benzyl alcohol as the analyte. The EOF of a new capillary was typically $\sim 1 \times 10^{-5}$ cm^2/Vs. If the residual EOF mobility is negligible in comparison with the mobilities of the analytes, as in the present case, the apparent mobilities can be calculated from the migration times, using eq 1

$$\mu = L_d/Et \quad (1)$$

where μ is the observed mobility, L_d is the distance to the detector (in cm), E is the electric field strength (in V/cm), and t is the time required for the sample to migrate to the detector (in seconds). The migration times were very reproducible: the average standard deviation of the mobility measured for a given sample on a given day was ± 0.2%. The average standard day-to-day variation of the mobility, using the same capillary, was typically ± 1.6%.

Each mobility profile was measured in a single capillary. However, it was occasionally necessary to change capillaries because of breakage or deterioration of the capillary coating. To compare the results obtained in different capillaries, it was necessary to correct for differences in the residual EOF of different capillaries. Because the EOF mobility and the analyte mobility are additive (*52*, *54*), the mobilities observed in the second and subsequent capillaries were corrected to the mobility that would have been observed in the original capillary using eq 2

$$\mu_{ss26,new\ cap} = \mu_{ss26,orig\ cap} + \Delta\mu \quad (2)$$

where $\mu_{ss26,new\ cap}$ is the observed mobility of ss26 (for example) in the new capillary, $\mu_{ss26,orig\ cap}$ is the observed mobility of ss26 in the original capillary, and $\Delta\mu$ is the difference between the mobilities observed in the two capillaries. The correction was typically less than 2% but ranged up to 20% for one of the capillaries. The corrected mobilities and the mobility profiles were always independent of the capillary in which the measurements were carried out.

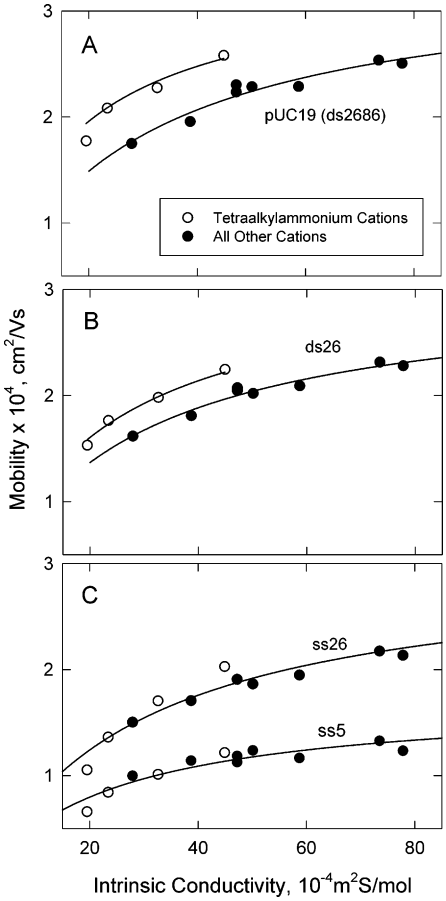

FIGURE 1: Dependence of the mobility of ss and dsDNA on the intrinsic conductivity of the cation in the solution. (A) Linear pUC19 (ds2686); (B) ds26; and (C) ss26 and ss5. All solutions contained 300 mM cation and a constant concentration of diethylmalonate as the anion. The open symbols correspond to solutions containing tetraalkylammonium cations: TMA^+, TEA^+, TPA^+, or TBA^+; the closed symbols refer to solutions containing Li^+, Na^+, K^+, Rb^+, $MeNH_3^+$, Me_3NH^+, $EtNH_3^+$, or $Tris^+$. The curved lines are rectangular hyperbolas that extrapolate to the origin and are meant to guide the eye.

RESULTS

Identification of Binding and Non-Binding Ions. To have an objective measure of which monovalent ions bind to DNA and which do not, the free solution mobilities of single- and double-stranded DNAs were measured in DM solutions of constant ionic strength containing different monovalent cations. Typical results are illustrated in Figure 1. The open circles correspond to the mobilities observed in solutions containing TMA^+, TEA^+, TPA^+, or TBA^+ as the cation, whereas the closed circles correspond to the mobilities observed when the counterion was an alkali metal ion (Li^+, Na^+, K^+, or Rb^+) or a partially substituted ammonium ion ($MeNH_3^+$, Me_3NH^+, $EtNH_3^+$, or $Tris^+$). In all cases, the mobility gradually increased as the limiting ionic conductivity of the cation at infinite dilution (hereafter called intrinsic conductivity for brevity) increased, as expected because the observed mobility of an analyte depends on the intrinsic conductivity of all of the ions in the solution (*55*, *56*). However, contrary to theory, the mobilities observed for dsDNA in solutions containing tetraalkylammonium ions are higher than those observed in solutions containing other cations with the same intrinsic conductivities. Because the mobilities observed for ss26 and ss5 are essentially inde-

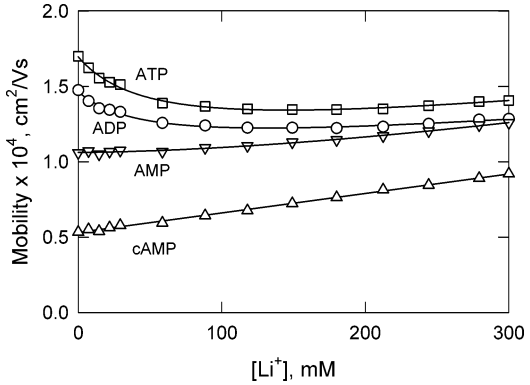

FIGURE 2: Mobility profiles observed for (□), ATP; (○), ADP; (▽), AMP; and (△), cAMP using Li^+ as the binding ion and TBA^+ as the non-binding ion. The straight line through the cAMP data was drawn by linear regression ($R^2 = 0.99$); the curved lines are drawn to guide the eye.

pendent of the type of cation in the solution, the mobility differences observed for dsDNA cannot be attributed to the effect of different cations on the hydrogen-bonded structure of water. Cation effects on water structure would be expected to affect the mobilities of single- and double-stranded DNAs in a similar manner (*57*). Hence, the dependence of the mobility of dsDNA on the type of monovalent cation in the solution suggests that dsDNA binds all (tested) monovalent cations except the quaternary ammonium ions, decreasing its effective net charge and reducing the observed mobility.

Very similar results have been observed with adenosine nucleotides (*44*). The mobilities observed for ATP, ADP, and AMP in solutions containing tetraalkylammonium ions are higher than those observed in solutions containing other cations with the same intrinsic conductivity, whereas the mobilities of cAMP and A-COOH are independent of the nature of the cation (*44*). Hence, ATP, ADP, and AMP bind all (tested) monovalent cations except the quaternary ammonium ions, in agreement with other results in the literature (*42*, *43*, *45*). On the basis of Figure 1 and for brevity in the following discussion, the tetraalkylammonium ions will be described as non-binding ions, whereas the other cations investigated in this study, Li^+, Na^+, K^+, NH_4^+, and $Tris^+$, will be described as binding ions, even though they do not bind to ssDNA, cAMP, or A-COOH. For brevity, the dependence of the observed mobility on the intrinsic conductivity of the cation in the solution will be called the conductivity effect.

Validation of the RI Method Using Adenosine Nucleotides as Analytes. To validate the RI method, the mobilities of ATP, ADP, and AMP were measured in solutions containing Li^+ as the binding ion, TPA^+ or TBA^+ as the non-binding ion, and cAMP as the non-binding analyte. The mobility profiles observed with TBA^+ as the non-binding ion are illustrated in Figure 2; similar results were obtained with TPA^+ (data not shown). The mobility of cAMP increases linearly with increasing $[Li^+]$ because of the conductivity effect, as expected because cAMP does not bind monovalent cations (*44*), and the intrinsic conductivity of Li^+ is greater than that of TBA^+ (*58*). In contrast, the mobilities of ATP and ADP decrease significantly with increasing $[Li^+]$ at the beginning of the titration because of counterion binding. However, at $[Li^+]$ above ~100 mM, the mobility goes through a shallow minimum and then begins to increase slowly as the conductivity effect becomes predominant. The mobility of AMP exhibits a very small decrease at low $[Li^+]$ and then increases nearly linearly with increasing $[Li^+]$ because of the conductivity effect; however, the slope of the line is smaller than that observed for cAMP.

The results in Figure 2 indicate that the mobility profiles observed for ATP, ADP, and AMP are the sum of two effects: a curvilinear decrease in mobility due to counterion binding and a linear increase (or decrease) in mobility due to the conductivity effect. To take both effects into account, the mobility profiles can be analyzed with eq 3

$$\mu_M = \mu_o - \frac{\Delta\mu_{span}[M^+]}{K_D + [M^+]} + c[M^+] \quad (3)$$

where μ_M is the mobility observed for the analyte−ligand complex at any given concentration $[M^+]$ of the test ion, μ_o is the mobility observed when $[M^+] = 0$ (i.e., when the solution contains only a tetraalkylammonium ion as the cation), $\Delta\mu_{span}$ is the span of the titration, (i.e., the difference in mobility that would be observed upon saturation of the binding site if there was no conductivity effect), K_D is the apparent dissociation constant characterizing the binding of the test ion to the analyte, and c is the slope of the line describing the conductivity effect. Binding, as used here, refers to the formation of a saturable complex between the analyte and ligand, assuming the binding to be non-cooperative.

Equation 3 contains three unknowns, $\Delta\mu$, K_D, and c, which can be determined by nonlinear curve fitting of the mobility profiles. However, the mobility profiles obtained from a typical experiment usually cover too small a range of ligand concentrations to accurately determine all three parameters (*44*). The parameter c in eq 3 can be eliminated if an analyte that does not bind the ligand is included in each solution. If the mobilities of the binding and non-binding analytes are different, subtracting the mobilities of the two analytes at each $[M^+]$ will give difference mobility profiles, which can be analyzed using eq 4.

$$\Delta\mu_M = \Delta\mu_o - \frac{\Delta\mu_{span}[M^+]}{K_D + [M^+]} \quad (4)$$

Here, $\Delta\mu_M$ is the difference in mobility between binding and non-binding analytes at a ligand concentration of $[M^+]$, $\Delta\mu_o$ is the value of $\Delta\mu_M$ when $[M^+] = 0$, and the other terms have been defined above. If the analyte has more than one independent binding site, additional terms corresponding to the second term on the right-hand side of eq 4 would be needed. However, attempts to fit the difference mobility profiles with more than one binding constant gave two nearly identical K_D values, indicating that multiple binding sites, if present, cannot be distinguished by the RI method. For this reason, the calculated K_D values are called apparent dissociation constants. All calculations were carried out using the SigmaPlot suite of programs.

The apparent K_D values calculated for the binding of Li^+ to ATP, ADP, and AMP, using TBA^+ as the non-binding ion and cAMP as the non-binding analyte, are given in Table 1. Similar results were obtained using TPA^+ as the non-binding ion (data not shown). The apparent K_D values, which

Table 1: Apparent K_D Values Calculated for ATP, ADP and AMP by the RI Method and Comparison with Literature Values[a]

analyte	apparent K_D, mM measured	apparent K_D, mM literature	references
ATP	82 ± 6	13−75	*42*−*44*, *59*, *60*
ADP	115 ± 14	71−109	*43*, *44*
AMP	373 ± 84	60−250	*43*, *44*, *61*

[a] Calculated from eq 4 using Li^+ as the binding ion, TBA^+ as the non-binding ion, and cAMP as the non-binding analyte. The uncertainties given for the K_D values are the standard errors of the residuals obtained from the SigmaPlot curve-fitting algorithm.

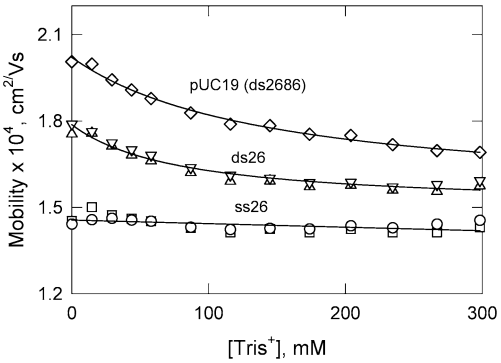

FIGURE 3: Mobility profiles observed for (◇) linear pUC19 (ds2686); (△,▽), ds26; and (○,□), ss26 using $Tris^+$ as the binding ion and TPA^+ as the non-binding ion. The two symbols for ds26 and ss26 represent independent runs on different days and illustrate the reproducibility of the method. The lines are drawn to guide the eye.

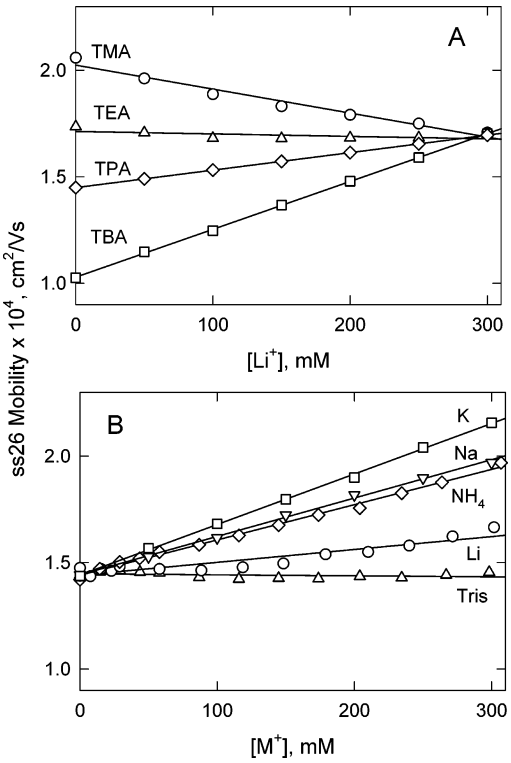

FIGURE 4: Dependence of the mobility of ss26, plotted as a function of binding ion concentration in solutions containing different replacement ion pairs. (A) Li^+ replacing the tetraalkylammonium ions: (○), TMA^+; (△), TEA^+; (◇), TPA^+; and (□), TBA^+. (B) TPA^+ replaced by (○), Li^+; (▽), Na^+; (□), K^+; (◇), NH_4^+; and (Δ), $Tris^+$. The total cation concentration was always 300 mM. The straight lines were drawn by linear regression, with correlation coefficients, $R^2 = 0.99$.

range from 82 to 373 mM for ATP, ADP, and AMP, respectively, are similar to the values obtained by pH titration (*42*, *43*, *59*), titration calorimetry (*60*), NMR (*61*), and capillary electrophoresis using the variable ionic strength (VIS) method (*44*). Hence, the RI method can accurately measure weak analyte−ligand binding constants.

The VIS and RI methods of determining binding constants are fundamentally different, even though both are based on capillary electrophoresis measurements. In the VIS method, the test ion is one of the components of the background electrolyte, and the differences in mobility between binding and non-binding analytes or between binding and non-binding ligands are measured as a function of ionic strength (*44*). The VIS method relies on the assumption that the binding constants are independent of ionic strength, whereas the RI method determines the affinity at a specific ionic strength. The two methods give similar results, as shown in Table 1.

Mobility Profiles Observed for Single- and Double-Stranded DNA. The mobility profiles observed for linear pUC19 (ds2686), ds26, and ss26, using $Tris^+$ as the binding ion and TPA^+ as the non-binding ion, are illustrated in Figure 3. The mobilities of pUC19 and ds26 decrease significantly with increasing [$Tris^+$], especially at low [$Tris^+$], because of counterion binding. The mobility of ss26 decreases slowly with increasing [$Tris^+$] because the intrinsic conductivity of $Tris^+$ is somewhat less than that of TPA^+ (*58*, *62*).

For other replacement ion pairs, the conductivity effect is more pronounced, as shown in Figure 4. With [Li^+] as the test ion, the mobility of ss26 increases or decreases substantially with increasing [Li^+], depending on whether the non-binding ion is TMA^+, TEA^+, TPA^+, or TBA^+ (Figure 4A). The slopes of the lines depend on whether the intrinsic conductivity of the particular tetraalkylammonium ion is greater or less than that of Li^+. Similarly, if the non-binding ion is TPA^+, the mobility of ss26 increases or decreases approximately linearly with increasing concentrations of K^+, Na^+, NH_4^+, Li^+, and $Tris^+$, as shown in Figure 4B. The correlation between the slopes of the lines in Figure 4 and the differences in the intrinsic conductivities of the binding and non-binding cations in each replacement ion pair is shown explicitly in Figure 5. The relatively good correlation between the two parameters indicates that the major factor contributing to the dependence of the mobility of a non-binding analyte on ligand concentration is the difference in the intrinsic conductivities of the replacement ion pair. However, the scatter of the data points suggests that secondary factors, such as the viscosity of the solution or the effect of the cation on the hydrogen-bonded structure of water (*57*), may also influence the observed mobilities.

Quantitative Analysis of Monovalent Counterion Binding by dsDNA. Because the mobility profiles obtained for ds26 and linear pUC19 were very similar (Figure 3), quantitative analysis of monovalent cation binding to dsDNA was carried out with ds26, using ss26 as the non-binding analyte. The difference mobility profiles obtained with Li^+ as the binding ion and TMA^+, TEA^+, TPA^+, or TBA^+ as the non-binding ion are shown in Figure 6A. With the first three quaternary ammonium ions, the difference mobility profiles are hyper-

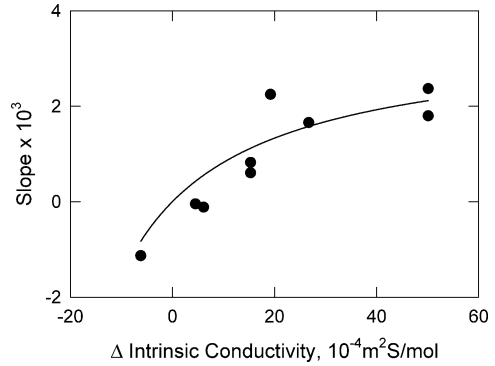

FIGURE 5: Analysis of the conductivity effect. The filled circles correspond to the slopes of the lines observed for ss26 in Figure 4, plotted as a function of the difference in the intrinsic conductivities of the replacement ion pair. The curved line is meant to guide the eye.

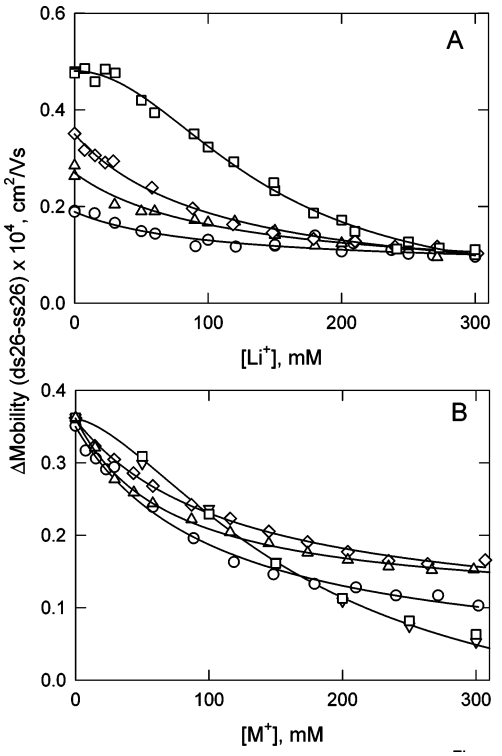

FIGURE 6: Difference mobility profiles calculated for ds26. (A) With Li^+ as the binding ion and (○), TMA^+; (△), TEA^+; (◇), TPA^+; and (□), TBA^+ as the non-binding ions. (B) With TPA^+ as the non-binding ion and (△), $Tris^+$; (○), Li^+; (▽), Na^+; (◇), NH_4^+; and (□), K^+ as the binding ions. The curved lines in (A) and (B) were calculated from eq 4 or 5, as described in the text, using the apparent K_D and cooperativity parameters given in Table 2.

bolic, as expected for non-cooperative binding between the analyte and ligand, allowing the apparent K_D values to be calculated from eq 4. However, with TBA^+ as the non-binding ion, the difference mobility profile exhibits a sigmoidal dependence on $[Li^+]$. Therefore, this difference mobility profile was analyzed using a four-parameter Hill equation (*63*)

$$\Delta\mu = \Delta\mu_o - \frac{\Delta\mu_{span}[M^+]^n}{K_D^n + [M^+]^n} \quad (5)$$

where n is the cooperativity parameter, and the other terms have been defined above. The apparent K_D values and the cooperativity parameters, n, obtained for Li^+ binding to ds26, using the four quaternary ammonium ions as the non-binding ions, are given in the top section of Table 2. The average apparent K_D value is 114 ± 18 mM, indicating that the binding affinity is essentially independent of the identity of the non-binding ion. Similar results have been observed for adenosine nucleotides (*44*).

Table 2: Apparent Dissociation Constants Obtained for ds26 Using Various Replacement Ion Pairs

binding ion	non-binding ion	apparent K_D, mM[a]	cooperativity, n	R^2
Li	TMA	100 ± 19		0.993
Li	TEA	108 ± 24		0.969
Li	TPA	107 ± 16		0.993
Li	TBA	140 ± 31	2.0 ± 0.2	0.998
Tris	TPA	71 ± 6		0.997
NH_4	TPA	120 ± 13		0.996
Li	TPA	107 ± 16		0.993
Na	TPA	173 ± 31	1.6 ± 0.2	0.998
K	TPA	173 ± 31	1.6 ± 0.2	0.998

[a] Calculated from eq 4 or 5 as described in the text.

The difference mobility profiles obtained for ds26 using TPA^+ as the non-binding ion and $Tris^+$, NH_4^+, Li^+, Na^+, and K^+ as the binding ions are illustrated in Figure 6B. The difference mobility profiles observed for the first three cations are hyperbolic and can be analyzed using eq 4. However, the difference mobility profiles observed for Na^+ and K^+ are sigmoidal and must be analyzed with eq 5. The apparent dissociation constants and cooperativity parameters obtained for the binding of $Tris^+$, NH_4^+, Li^+, Na^+, and K^+ to ds26 are given in the bottom section of Table 2. The apparent K_D values range from 71 to 173 mM, indicating that all five cations bind weakly to ds26 and, most likely, to other dsDNAs. The ratios of the apparent K_D values obtained for the binding of the alkali metal ions Li^+, Na^+, and K^+ to ds26 are 0.62:l.00:1.00, respectively, similar to the ratios of 0.67:1.00:1.25 observed by Ross and Scruggs for the same three cations binding to calf thymus DNA (*1*). The apparent K_D values measured for the binding of Na^+ and K^+ to ds26, 173 mM, are significantly larger than the value of 71 μM determined by Ouameur et al. (*9*) for the binding of thallium to calf thymus DNA. However, these two results should not be quantitatively compared because the binding ions are different, and the experimental conditions were also very different. The apparent K_D values reported for ds26 in Table 2 are similar to the values observed for the binding of the same cations to ATP and ADP (Table 1), as might be expected for ligands binding to similar analytes.

DISCUSSION

The replacement ion (RI) method described in this article is a method for measuring weak binding affinities by capillary electrophoresis using very small quantities of analyte. The experiments are carried out at constant ionic strength by gradually replacing a non-binding ion in the solution with the test ion. To compensate for the dependence of the observed mobility on the intrinsic conductivities of different ions, the mobilities of binding and non-binding analytes are measured in the same solution at each test ion concentration. The difference mobility profiles are then analyzed by nonlinear curve fitting, using eq 4 or 5 to

calculate the apparent dissociation constants, depending on whether the binding isotherms are hyperbolic or sigmoidal. Binding and non-binding ions with similar intrinsic conductivities can be used to minimize the conductivity effect. However, as shown in Table 2, the calculated apparent K_D values are essentially independent of the particular non-binding ion used, indicating that the difference mobility profiles adequately correct for the conductivity effect.

The results in Table 2 also indicate that monovalent cations bind weakly to dsDNA, with apparent dissociation constants ranging from 71 to 173 mM. These results, together with other studies in the literature (*1*−*9*), suggest that all, or nearly all, monovalent cations bind to random-sequence dsDNA in aqueous solutions. The apparent K_D observed for the binding of $Tris^+$ to ds26 is somewhat smaller than that observed for the binding of other cations, suggesting that Tris−DNA complexes are stabilized by the formation of hydrogen bonds with the DNA bases (*45*) as well as by electrostatic interactions with the phosphate residues. Because of the similarity of the binding constants, positively charged $Tris^+$ buffer ions will compete with other monovalent cations for binding to dsDNA in Tris-buffered solutions.

Counterion binding, as measured in the present study, implies the formation of saturable cation−dsDNA complexes, which in turn implies the site-binding of cations to random-sequence dsDNA. The site-binding of monovalent counterions to random-sequence dsDNA has previously been suggested from circular dichroism (*64*) and thermal melting (*65*) studies. Site-bound cations are different from the condensed counterions that surround dsDNA because of its high linear charge density (*66*). Condensed counterions are territorially bound to the whole DNA molecule; the concentration of the condensed cations is nearly independent of the bulk cation concentration (*66*, *67*). In contrast, the concentration of the bound cations described here increases with increasing cation concentration, even though the total ionic strength of the solution is held constant.

Recently, a new theory was proposed to describe the interaction between DNA and its counterions called the tightly bound ion (TBI) theory (*68*−*70*). This theory separates the condensed counterion layer described by Manning (*66*) into two regions, one containing tightly bound ions and the other containing diffusively bound ions. The strongly correlated, tightly bound ions are trapped in discrete but unspecified locations (called tightly bound cells) on the DNA surface by the strong electrostatic field of the phosphate residues. Importantly, the number of tightly bound ions increases with increasing cation concentration and approaches saturation at high cation concentrations. The diffusively bound ions are weakly correlated and form an outer layer around the DNA and the tightly bound ions; the diffusively bound ions in this outer layer can be described by the Poisson−Boltzmann theory. The rest of the cations are found in the bulk phase and contribute to the ionic strength of the solution (*68*−*70*).

The tightly bound ions in the TBI theory appear to correspond to the bound cations in the present study because the concentration of the tightly bound ions increases with increasing cation concentration and approaches saturation at high cation concentrations, as observed here. The nature of the binding site(s) is not known, although circular dichroism studies have suggested that alkali metal ions bind to guanine residues in the minor groove, causing an increase in the average winding angle of the helix backbone (*64*). Monovalent cation binding appears to approach saturation when the DNA is still negatively charged, suggesting that a minimal charge density is needed for cations to bind to dsDNA. The importance of charge density is underscored by the absence of monovalent cation binding to ssDNA, cAMP, and A-COOH under conditions where significant binding is observed with dsDNA, ATP, ADP, and AMP. Further studies will be needed to determine how monovalent cation binding depends on DNA charge density.

The present study does not address the binding of monovalent cations to specific DNA sequences such as A-tracts because ds26 and linear pUC19 have essentially random sequences. One would expect the site-binding of monovalent cations in the A-tract minor groove, for example, to occur in addition to the non-sequence-specific binding described here. The site-binding of monovalent cations to DNA A-tracts will be described in a future communication (manuscript in preparation).

REFERENCES

1. Ross, P. D., and Scruggs, R. L. (1964) Electrophoresis of DNA. II. Specific interactions of univalent and divalent cations with DNA, *Biopolymers 2*, 79−89.
2. Ross, P. D., and Scruggs, R. L. (1964) Electrophoresis of DNA. III. The effect of several univalent electrolytes on the mobility of DNA, *Biopolymers 2*, 231−236.
3. Strauss, U. P., Helfgott, D., and Pink, H. (1967) Interactions of polyelectrolytes with simple electrolytes. II. Donnan equilibria obtained with DNA in solutions of 1-1 electrolytes, *J. Phys. Chem. 71*, 2550−2556.
4. Shapiro, J. T., Stannard, B. S., and Felsenfeld, G. (1969) The binding of small cations to deoxyribonucleic acid. Nucleotide specificity, *Biochemistry 8*, 3233−3241.
5. Anderson, C. F., Record, M. T., Jr., and Hart, P. A. (1978) Sodium-23 NMR studies of cation-DNA interactions, *Biophys. Chem. 7*, 301−316.
6. Korolev, N., Lyubartsev, A. P., Rupprecht, A., and Nordenskiöld, L. (1999) Experimental and Monte Carlo simulation studies on the competitive binding of Li^+, Na^+ and K^+ ions to DNA in oriented DNA fibers, *J. Phys. Chem. B 103*, 9008−9019.
7. Tikhomirova, A., and Chalikian, T. V. (2004) Probing hydration of monovalent cations condensed around polymeric nucleic acids, *J. Mol. Biol. 341*, 551−563.
8. Gearheart, L. A., Somoza, M. M., Rivers, W. E., Murphy, C. J., Coleman, R. S., and Berg, M. A. (2003) Sodium-ion binding to DNA: detection by ultrafast time-resolved Stokes-shift spectroscopy, *J. Am. Chem. Soc. 125*, 11812−11813.
9. Ouameur, A. A., Nafisi, Sh., Mohajerani, N., and Tajmir-Riahi, H. A. (2003) Thallium-DNA complexes in aqueous solution. Major or minor groove binding, *J. Biomol. Struct. Dyn. 20*, 561−565.
10. Shui, X., Sines, C. C., McFail-Isom, L., VanDerveer, D., and Williams, L. D. (1998) Structure of the potassium form of CGCGAATTCGCG: DNA deformation by electrostatic collapse around inorganic cations, *Biochemistry 37*, 16877−16887.
11. Tereshko, V., Minasov, G., and Egli, M. (1999) A "Hydrat-ion" spine in a B-DNA minor groove, *J. Am. Chem. Soc. 121*, 3590−3595.
12. Woods, K. K., McFail-Isom, L., Sines, C. C., Howerton, S. B., Stephens, R. K., and Williams, L. D. (2000) Monovalent cations sequester within the A-tract minor groove of [d(CGCGAATTCGCG)], *J. Am. Chem. Soc. 122*, 1546−1547.
13. Sines, C. C., McFail-Isom, L., Howerton, S. B., VanDerveer, D., and Williams, L. D. (2001) Cations mediate B-DNA conformational heterogeneity, *J. Am. Chem. Soc. 122*, 11048−11056.
14. Howerton, S. B., Sines, C. C., VanDerver, D., and Williams, L. D. (2001) Locating monovalent cations in the grooves of B-DNA, *Biochemistry 40*, 10023−10031.

15. Hud, N. V., Sklenář, V., and Feigon, J. (1999) Localization of ammonium ions in the minor groove of DNA duplexes in solution and the origin of DNA A-tract bending, *J. Mol. Biol. 186*, 651−660.
16. MacDonald, D., Herbert, K., Zhang, X., Polgruto, T., and Lu, P. (2001) Solution structure of an A-tract bend, *J. Mol. Biol. 306*, 1081−1098.
17. Barbič, A., Zimmer, D. P., and Crothers, D. M. (2003) Structural origins of adenine-tract bending, *Proc. Natl. Acad. Sci. U.S.A. 100*, 2369−2373.
18. Wu, A., Delaglio, F., Tjandra, N., Zhurkin, V. B., and Bax, A. (2003) Overall structure and sugar dynamics of a DNA dodecamer from homo- and heteronuclear dipolar couplings and ^{31}P chemical shift anisotropy, *J. Biomol. NMR 26*, 297−315.
19. Marincola, F. C., Denisov, V. P., and Halle, B. (2004) Competitive Na^+ and Rb^+ binding in the minor groove of DNA, *J. Am. Chem. Soc. 126*, 6739−6750.
20. Stefl, R., Wu, H., Ravindranathan, S., Sklenář, V., and Feigon, J. (2004) DNA A-tract bending in three dimensions: solving the dA_4T_4 vs. dT_4A_4 conundrum, *Proc. Natl. Acad. Sci. U.S.A. 101*, 1177−1182.
21. Tóth, K., Sauermann, V., and Langowski, J. (1998) DNA curvature in solution measured by fluorescence resonance energy transfer, *Biochemistry 37*, 8173−8179.
22. Strauss, J. K., and Maher, L. J., III. (1994) DNA bending by asymmetric phosphate neutralization, *Science 266*, 1829−1834.
23. Stellwagen, N. C., Magnusdóttir, S., Gelfi, C., and Righetti, P. G. (2001) Preferential counterion binding to A-tract DNA oligomers, *J. Mol. Biol. 305*, 1025−1033.
24. Young, M. A., Jayaram, B., and Beveridge, D. L. (1997) Intrusion of counterions into the spine of hydration in the minor groove of B-DNA: fractional occupancy of electronegative pockets, *J. Am. Chem. Soc. 119*, 59−69.
25. Feig, M., and Pettit, B. M. (1999) Sodium and chlorine ions as part of the DNA solvation shell, *Biophys. J. 77*, 1769−1781.
26. Hammelberg, D., McFail-Isom, L, Williams, L. D., and Wilson, W. D. (2000) Flexible structure of DNA: ion dependence of minor-groove structure and dynamics, *J. Am. Chem. Soc. 122*, 10513−10520.
27. Korolev, N., Lyubartsev, A. P., Laaksonen, A., and Nordenskiöld, L. (2002) On the competition between water, sodium ion, and spermine in binding to DNA: a molecular dynamics computer simulation study, *Biophys. J. 82*, 2860−2875.
28. Mocci, F., and Saba, G. (2003) Molecular dynamics simulations of A·T-rich oligomers: sequence-specific binding of Na^+ in the minor groove of B-DNA, *Biopolymers 68*, 471−485.
29. Korolev, N., Lyubartsev, A. P., Laaksonen, A., and Nordenskiöld, L. (2003) A molecular dynamics simulation study of oriented DNA with polyamine and sodium counterions: diffusion and averaged binding of water and cations, *Nucleic Acids Res. 31*, 5971−5981.
30. Várnai, P., and Zakrzewska, K. (2004) DNA and its counterions: a molecular dynamics study, *Nucleic Acids Res. 32*, 4269−4280.
31. Ponomarev, S. Y., Thayer, K. M., and Beveridge, D. L. (2004) Ion motions in molecular dynamics simulations on DNA, *Proc. Natl. Acad. Sci. U.S.A. 101*, 14771−14775.
32. Rueda, M., Cubero, E., Laughton, C. A., and Orozco, M. (2004) Exploring the counterion atmosphere around DNA: what can be learned from molecular dynamics simulations? *Biophys. J. 87*, 800−811.
33. Olson, W. K., and Zhurkin, V. B. (1995) Twenty Years of DNA Bending, in *Biological Structure and Dynamics* (Sarma, R. H., and Sarma, M. H., Eds.) pp 341−370, Adenine Press, Schenectedy, NY.
34. McFail-Isom, L., Sines, C. C., and Williams, L. D. (1999) DNA structure: cations in charge? *Curr. Opin. Struct. Biol. 9*, 298−304.
35. Williams, L. D., and Maher, L. J., III. (2000) Electrostatic mechanisms of DNA deformation, *Annu. Rev. Biophys. Biomol. Struct. 29*, 497−521.
36. Hud, N. V., and Plavec, J. (2003) A unified model for the origin of DNA sequence-directed curvature, *Biopolymers 69*, 144−159.
37. Manning, G. S. (2006) The contribution of transient counterion imbalances to DNA bending fluctuations, *Biophys. J. 90*, 3208−3215.
38. Range, K., Mayaan, E., Maher, L. J., III, and York, D. M. (2005) The contribution of phosphate-phosphate repulsions to the free energy of DNA bending, *Nucleic Acids Res. 33*, 1257−1268.
39. Shikiya, R., Li, J.-S., Gold, B., and Marky, L. A. (2005) Incorporation of cationic chains in the Dickerson-Drew dodecamer: correlation of energetics, structure and ion and water binding, *Biochemistry 44*, 12582−12588.
40. Williams, S. L., Parkhurst, L. K., and Parkhurst, L. J. (2006) Changes in DNA bending and flexing due to tethered cations detected by fluorescence resonance energy transfer, *Nucleic Acids Res. 34*, 1028−1035.
41. Strauss, J. K., Roberts, C., Nelson, M. G., Switzer, C., and Maher, L. J., III. (1996) DNA bending by hexamethylene-tethered ammonium ions, *Proc. Natl. Acad. Sci. U.S.A. 93*, 9515−9520.
42. Smith, R. M., and Alberty, R. A. (1956) The apparent stability constants of ionic complexes of various adenosine phosphates with monovalent cations, *J. Phys. Chem. 60*, 180−184.
43. Smith, R. M., Martell, A. E., and Chen, Y. (1991) Critical evaluation of stability constants for nucleotide complexes with protons and metal ions and the accompanying enthalpy changes, *Pure Appl. Chem. 63*, 1015−1080.
44. Stellwagen, E., and Stellwagen, N. C. (2006) Quantitative analysis of cation binding to the adenosine nucleotides using the variable ionic strength (VIS) method: validation of the Debye-Hückel-Onsager theory of electrophoresis in the absence of counterion binding, *Electrophoresis*, *28*, in press.
45. Sigel, H., and Griesser, R. (2005) Nucleoside 5′-triphosphates: self-association, acid-base, and metal ion-binding properties in solution, *Chem. Soc. Rev. 34*, 875−900.
46. Heegaard, N. H. H., and Kennedy, R. T. (1999) Identification, quantitation, and characterization of biomolecules by capillary electrophoretic analysis of binding interactions, *Electrophoresis 20*, 3122−3133.
47. Tanaka, Y., and Terabe, S. (2002) Estimation of binding constants by capillary electrophoresis, *J. Chromatogr., B 768*, 81−92.
48. Li, D., Fu, S., and Lucy, C. A. (1999) Prediction of electrophoretic mobilities. 3. Effect of ionic strength in capillary zone electrophoresis, *Anal. Chem. 71*, 687−699.
49. Jouyban, A., and Kenndler, E. (2006) Theoretical and empirical approaches to express the mobility of small ions in capillary electrophoresis, *Electrophoresis 27*, 992−1005.
50. Stellwagen, E., and Stellwagen, N. C. (2002) The free solution mobility of DNA in Tris-acetate-EDTA buffers of different concentrations, with and without added NaCl, *Electrophoresis 23*, 1935−1941.
51. Stellwagen, E., and Stellwagen, N. C. (2003) Probing the electrostatic shielding of DNA with capillary electrophoresis, *Biophys. J. 84*, 1855−1866.
52. Stellwagen, N. C., Gelfi, C., Righetti, P. G. (1997) The free solution mobility of DNA, *Biopolymers 42*, 687−703.
53. Williams, B. A., and Vigh, G. (1995) Fast, accurate mobility determination method for capillary electrophoresis, *Anal. Chem. 68*, 1174−1180.
54. Grossman, P. D. (1992) Factors Affecting the Performance of Capillary Electrophoresis Separations: Joule Heating, Electroosmosis, and Zone Dispersion, in *Capillary Electrophoresis, Theory and Practice* (Grossman, P. D., and Colburn, J. D., Eds.) pp 3−43, Academic Press, San Diego, CA.
55. Bockris, J. O'M., and Reddy, A. K. N. (1998) *Modern Electrochemistry*, 2nd ed., Vol. 1, Plenum Press, New York.
56. Manning, G. S. (1981) Limiting laws and counterion condensation in polyelectrolyte solutions. 7. Electrophoretic mobility and conductance, *J. Phys. Chem. 85*, 1506−1515.
57. Stellwagen, E., Dong, Q., and Stellwagen, N. C. (2005) Monovalent cations affect the free solution mobility of DNA by perturbing the hydrogen-bonded structure of water, *Biopolymers 78*, 62−68.
58. Weast, R. C., Ed. (1984) *CRC Handbook of Chemistry and Physics*, 65th ed., pp D171−D172, CRC Press, Boca Raton, FL.
59. Botts, J., Chasin, A., and Young, H. L. (1965) Alkali metal binding by ethylenediaminetetraacetate, adenosine 5′-triphosphate, and pyrophosphate, *Biochemistry 4*, 1788−1796.
60. Wilson, J. E., and Chin, A. (1991) Chelation of divalent cations by ATP, studied by titration calorimetry, *Anal. Biochem. 193*, 16−19.
61. Haake, P., and Prigodich, R V. (1984) Method for determination of phosphate anion-cation association constants from ^{31}P chemical shifts, *Inorg. Chem. 23*, 457−462.
62. Klein, S. D., and Bates, R. G. (1980) Conductance of tris-(hydroxymethyl)aminomethane hydrochloride (Tris·Cl) in water at 25 and 37°C, *J. Solution Chem. 9*, 289−292.
63. Wyman, J., and Gill, S. J. (1990) *Binding and Linkage*, University Science Books, Mill Valley, CA.

64. Kilkuskie, R., Wood, N., Ringquist, S., Shinn, R., and Hanlon, S. (1988) Effects of charge modification on the helical period of duplex DNA, *Biochemistry 27*, 4377−4386.
65. Owczarzy, R., Dunietz, I., Behlke, M. A., Klotz, I. M., and Walder, J. A. (2003) Thermodynamic treatment of oligonucleotide duplex-simplex equilibria, *Proc. Natl. Acad. Sci. U.S.A. 100*, 14840−14845.
66. Manning, G. S. (1978) The molecular theory of polyelectrolyte solutions with applications to the electrostatic properties of polynucleotides, *Q. Rev. Biophys. 11*, 179−246.
67. Record, M. T., Jr., Anderson, C. F., and Lohman, T. M. (1978) Thermodynamic analysis of ion effects on the binding and conformational equilibria of proteins and nucleic acids: the roles of ion association or release, screening, and ion effects on water activity, *Q. Rev. Biophys. 11*, 103−178.
68. Tan, Z.-J, and Chen, S.-J. (2005) Electrostatic correlations and fluctuations for ion binding to a finite length polyelectrolyte, *J. Chem. Phys. 122*, 044903.
69. Tan, Z.-J., and Chen, S.-J. (2006) Nucleic acid helix stability: effects of salt concentration, cation valence and size, and chain length, *Biophys. J. 90*, 1175−1190.
70. Tan, Z.-J., and Chen, S.-J. (2006) Ion-mediated nucleic acid helix-helix interactions, *Biophys. J. 91*, 518−536.

BI062132W